Thermochimica Acta 472 (2008) 31–37

Contents lists available at ScienceDirect

Thermochimica Acta

journal homepage: www.elsevier.com/locate/tca

A study of the thermo-mechanical behavior of Boehmite-polyamide-6 nanocomposites

Ceren Özdilek*, Ben Norder, Stephen J. Picken

NanoStructured Materials, Delft University of Technology, Julianalaan 136, 2826 BL, Delft, The Netherlands

ARTICLE INFO

Article history:
Received 20 December 2007
Received in revised form 3 March 2008
Accepted 13 March 2008
Available online 22 March 2008

Keywords:
Nanocomposite
Boehmite
Heat distortion temperature
Glass transition temperature
Thermo-oxidative stability

ABSTRACT

Some of the important thermo-mechanical characteristics of Boehmite-polyamide-6 nanocomposites are presented. Two different types of Boehmite (γ-AlOOH) are investigated, which are unmodified and surface-modified using a titanate-coupling agent. Since use-temperature range is one of the most important parameters for engineering polymers, heat distortion temperature (HDT) and glass transition temperature (T_g) of the nanocomposites are analyzed in detail. According to the dynamic mechanical analysis (DMA), both storage and loss modulus show a gradual increase with (Ti-)Boehmite concentration. Compared to the HDT of the unfilled polymer (67 °C), there is a tremendous increase in HDTs of the nanocomposites up to 143 and 155 °C at 9% Boehmite and 15% Ti-Boehmite contents, respectively. PA6-Boehmite samples show a random variation in T_g values whereas the PA6-Ti-Boehmite samples have a certain trend: T_g values gradually decrease in the beginning, and then increase with filler concentration. It is shown that both series of nanocomposites have similar thermo-oxidative stabilities. Therefore, both the trend in T_gs and the lower HDT values at low Ti-Boehmite contents are attributed to the plasticizing effect of the titanate-coupling agent. Complex Halpin–Tsai model has been used to assess the temperature-dependent mechanical properties of the nanocomposites.

1. Introduction

Polymer nanocomposites form a special and relatively new class of composites that are characterized by a dispersed phase with (at least) one length scale in the nanometer range. Therefore, they possess a large interfacial area per unit volume or weight of the dispersed phase (about 750 m^2/g) [1]. Due to this large interface, nanocomposites can demonstrate significant improvements in polymer properties compared to conventional composites in terms of: mechanical properties; such as increased stiffness, tensile and/or compressive strength; barrier properties, such as increased chemical and/or heat resistance; other interesting features including dimensional stability and optical homogeneity. Also it should be noted that these improvements can be obtained at 1–10 wt.% nano-filler contents, which are much lower than the typical filler contents in conventional (micro) composites. Since the nano-filler contents are generally below 10%; material costs are lowered and the nanocomposite products become lighter than conventional microcomposite products.

The first well-defined polymer nanocomposites were developed by the Toyota researchers in 1987 [2]. In a series of studies, ε-caprolactam was polymerized within silicate layers of organically modified clays thereby forming polyamide-6-clay nanocomposites. It was observed that upon addition of only 4.2% clay, the storage modulus doubled, the strength increased more than 50%, and the heat distortion temperature increased by 80 °C compared to the pristine polymer [3,4]. These polyamide-6-clay nanocomposites also demonstrated significant improvements in dimensional stability, barrier properties and flame retardance [5,6]. Since then, many different polymers and nano-fillers have been investigated for similar purposes. Some of the well-known nano-filler systems and geometries are summarized as follows: silica, carbon black (spherical); boehmite, sepiolite (rod-shaped); kaolinite, mica, bayerite, gibbsite (plate-shaped); hectorite, montmorillonite, saphonite, laponite (layered); synthetic fibres, carbon nanotubes (fibrous) [7]. Among these, the most studied ones are the layered silicates, while there are fewer nanocomposite studies involving inorganic colloidal systems (plate- or rod-shaped). Research on nanocomposites containing carbon nanotubes and synthetic fibres is in a development stage.

In our previous work, we have described a procedure for obtaining polyamide-6 nanocomposites containing colloidal Boehmite particles [8,9]. Boehmite, which is also known as γ-AlOOH, is a

* Corresponding author. Tel.: +32 16 322362; fax: +32 16 322991.
E-mail address: Ceren.Ozdilek@cit.kuleuven.be (C. Özdilek).

0040-6031/$ – see front matter © 2008 Elsevier B.V. All rights reserved.
doi:10.1016/j.tca.2008.03.008

rod-like system with an orthorhombic single crystal structure. Our past studies have focused on the effects of Boehmite on mechanical properties and polymer morphology in its nanocomposites. It has been shown that the polymer crystalline structure is significantly changed and the storage modulus is effectively doubled upon inclusion of Boehmite particles. Although the positive effect of Boehmite on the storage modulus is obvious, these nanocomposites require further optimization before they can be used in engineering applications.

This paper presents some of the important thermo-mechanical properties of the Boehmite-polyamide-6 system, which have not been reported before. These properties influence profoundly the performance of engineering materials. The use-temperature range is one of the most important parameters for engineering polymers and therefore, heat distortion and glass transition temperatures deserve special attention as much as thermo-oxidative stabilities. In this paper, polyamide-6 containing two different types of filler (unmodified and surface-modified Boehmite) are discussed. The Halpin–Tsai model, which has been used in our previous work to explain the mechanical properties of the nanocomposites at room temperature, is used also here for predicting these properties as a function of temperature. With this approach, it is possible to obtain the model predictions for heat distortion and glass transition temperatures and compare them to the experimental ones.

2. Experimental

2.1. Synthesis

Boehmite particles were synthesized according to the method of Buining et al. [10]. This method yielded colloidal Boehmite rods dispersed in an aqueous medium, with average dimensions of 280 nm (length) and 20 nm (width). These dimensions could contain up to 30% of polydispersity. For the surface-modification of Boehmite particles, a titanate type of coupling agent named as titanium IV, tris[2-[(2-aminoethyl)amino]ethanolato-*O*],2-propanolato was used. (KR-44, Kenrich Chemicals). Prior to the surface treatment, Boehmite particles were transferred into *n*-propanol because of the poor solubility of the coupling agent in water. In the end, transparent and very stable dispersions of titanate-modified Boehmite in *n*-propanol were obtained. Further information on the Boehmite synthesis and the surface modification method can be found in our previous articles [8,9].

Preparation of the nanocomposites was carried out via ring-opening polymerization of ε-caprolactam in a melt polymerization set-up. In this scheme, the reaction was initiated by water via opening of the caprolactam ring and production of aminocaproic acid. Propagation took place by reaction of the generated amino acid with the cyclic monomer. The monomer, ε-caprolactam (Fluka) and the other reactants were used without further purification. The relative amounts of reactants were the following: 40 g ε-caprolactam, 10 g aminocaproic acid, 0.25 g adipic acid and 10 ml demineralized water. All reactions were carried out in a 500-ml glass polymerization vessel equipped with an automatic stirrer and a temperature controller. The reaction mixture was heated at 150 °C for 2 h to remove excess of water, which was followed by polymerization at 230 °C during 4 h. The polymer product in melt was poured out of the reactor and was subjected to Soxhlet extraction in methanol for 12 h, in order to remove unreacted monomers and cyclic/linear oligomers. Upon inclusion of unmodified and titanate-modified Boehmite dispersions in the polymerization, two different types of polyamide-6 nanocomposites were obtained. These nanocomposites contained 1, 1.3, 5, 7.5, and 9% Boehmite; and 1, 3, 5.5, 7, 13, and 15% Ti-Boehmite, respectively (as weight percentages).

2.2. Sample preparation

For characterization, the nanocomposite samples were pressed into thin films of about 0.3 mm by using a hydraulic polymer-melt press. The temperature of the press was 250 °C and the applied force was approximately 180 kN. The films were extensively dried and stored in a vacuum oven at 80 °C.

2.3. Thermogravimetric analysis

Boehmite contents and thermo-oxidative stabilities of the nanocomposites were determined by thermogravimetric analysis (TGA) performed by a PerkinElmer TGA-7 Thermal Gravimetric Analyzer. For determination of the exact Boehmite contents, the samples were heated from 25 to 800 °C at a rate of 50 °C/min under a N_2 atmosphere and were held at this temperature for 30 min. As the polymer degraded completely at 800 °C, the residual weight was related to the inorganic content. The weight change of the freeze-dried particles (Boehmite and titanate-modified Boehmite) due to loss of water in the crystalline structure and the weight loss of the surface modifier were measured in TGA and were taken into account in the calculations. For thermo-oxidative stabilities, the measurements were done in the temperature range 25–700 °C at a rate of 10 °C/min under an air atmosphere. Some of the measurements were repeated to check reproducibility, but finally, the values from single measurements were used in constructing the TGA curves instead of the averages.

2.4. Dynamic mechanical analysis (DMA)

Storage and loss modulus of the nanocomposites were measured in the extension mode at a frequency of 1 Hz by using a PerkinElmer DMA 7e Dynamical Mechanical Analyzer. The signal amplitude was in the range of 5–8 μm. The measurements were done in the interval 25–160 °C, at a heating/cooling rate of 5 °C/min and under a N_2 atmosphere. Each one of the pressed polymer films was cut into a small rectangle of 9–7 mm long and 2.5 mm wide. As mentioned before, the film thickness was about 0.3 mm after pressing.

3. Results and discussion

3.1. Heat distortion temperature

As indicated in Section 2.4, storage modulus of the nanocomposites was measured during both heating and cooling, in the temperature range of 25–160 °C. The modulus values obtained in the cooling part of the curves were higher compared to those of the heating part, probably due to some slight improvement in crystallinity and/or orientation during the extension measurements. Therefore, the main focus will be on the cooling part of the modulus curves for all samples: in Figs. 1 and 2, the storage modulus results of PA6-Boehmite and PA6-Ti-Boehmite samples are shown as a function of temperature (in the interval 37–160 °C). Upon increasing the Boehmite (Ti-Boehmite) content, the storage modulus gradually increases. In the end, it reaches 3.74 and 4.23 GPa at 9% Boehmite and 15% Ti-Boehmite contents, respectively. Compared to the melt-polymerized unfilled polyamide-6, a doubling of the storage modulus is observed. The storage modulus improvement as summarized above, was reported earlier in our previous work [8,9].

An important parameter that can be derived from storage modulus—temperature curves is the heat distortion temperature (HDT). The HDT of a polymeric material is a measure of its heat resistance under applied constant stress. In the standard testing method (ASTM D648), materials are subjected to a constant flexural

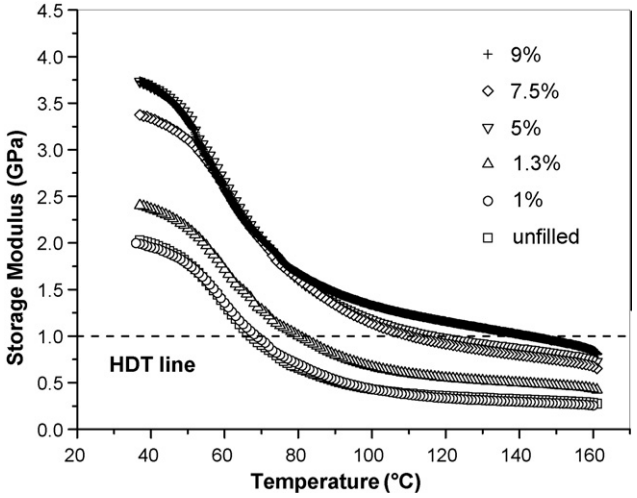

Fig. 1. Storage modulus E' curves of PA6-Boehmite samples in the temperature interval 37–160 °C, measured at 1 Hz.

load of 455 or 1802 Pa and heated at a rate of 2 °C/min. The modulus of the polymer decreases with increasing temperature and it reaches a critical modulus value at which a deflection of 0.25 mm is observed. The temperature corresponding to the deflection point is recorded as the HDT of the polymer. Apart from the standard testing method, storage modulus—temperature curves can also be used to obtain the same kind of information. In the literature, there is a large variation in reference values that are used in HDT determination. According to our reference, the HDT is the temperature at which the storage modulus reaches 1 GPa or 250 MPa [11]. In our case, the HDT values were determined from the storage modulus curves (Figs. 1 and 2) in accordance with this reference, as the points at which the modulus curves intersect the 1 GPa line. HDT's of the PA6-Boehmite and PA6-Ti-Boehmite samples are presented in Table 1.

In PA6-Boehmite samples, the HDT increases gradually from 67 °C for the unfilled polyamide-6 to 143 °C for the nanocomposite with 9% Boehmite (Table 1). On the other hand, it does not increase immediately with PA6-Ti-Boehmite samples. In the beginning, HDT attains values lower than that of the unfilled polymer at Ti-Boehmite contents of 1–5.5%. This effect can be explained by the presence of the flexible surface-modifying agent in these samples, which probably acts as a plasticizer. This plasticizing effect will be revisited in the next section. Starting from 7% Ti-Boehmite content, the effect is counter-balanced by the presence of more filler particles so that the HDT starts to increase. In this series, the highest HDT value is reached at 15% Ti-Boehmite content (155 °C). Among various polymer-inorganic filler nanocomposites reported in the literature, polyamide-6-clay systems show the most dramatic improvement in HDT. It has been reported that the HDT of a polyamide-6-clay system undergoes an increase from 65 °C of the pure polymer to 145 °C of the nanocomposite at 4.2 wt% clay loading [12]. Indeed, the HDT increments of our nanocomposites at 5% Boehmite and 5.5% Ti-Boehmite contents are lower compared to that particular polyamide-6-clay system. This observation is in agreement with our previous conclusion that Boehmite particles provide less constraint on the polymer chains in comparison to clay platelets [8]. Therefore less dramatic improvements in HDT should be expected from Boehmite nanocomposites. At the highest Boehmite contents, HDT increments of PA6-Boehmite and PA6-Ti-Boehmite are 76 and 88 °C, respectively (Table 1). These increments are quite significant, but they occur at much higher filler concentrations in comparison to polyamide-6-layered silicate (clay) nanocomposites. Considering the rod like shape of the Boehmite particles we anticipate a smaller effect of Boehmite nanoparticles on the barrier properties of PA6.

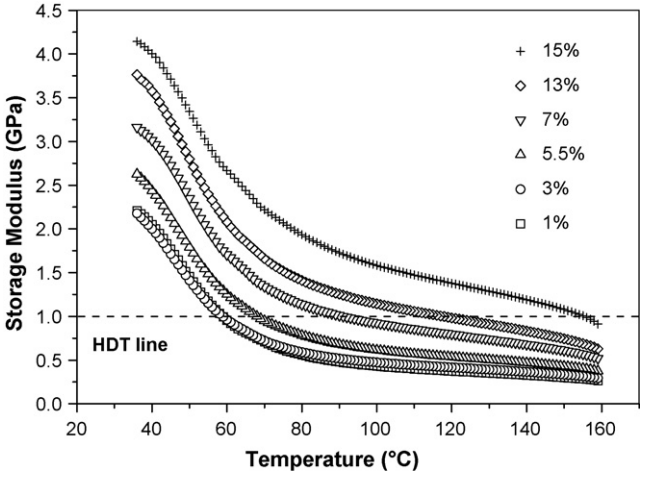

Fig. 2. Storage modulus E' curves of PA6-Ti-Boehmite samples in the temperature interval 37–160 °C, measured at 1 Hz.

Table 1
Heat distortion temperatures of PA6-Boehmite and PA6-Ti-Boehmite

Sample	HDT at 1 GPa (°C)
PA6-unfilled	67
PA6-Boeh 1%	68
PA6-Boeh 1.3%	80
PA6-Boeh 5%	117
PA6-Boeh 7.5%	110
PA6-Boeh 9%	143
PA6-Ti-Boeh 1%	58
PA6-Ti-Boeh 3	58
PA6-Ti-Boeh 5.5%	68
PA6-Ti-Boeh 7%	91
PA6-Ti-Boeh 13%	117
PA6-Ti-Boeh 15%	155

3.2. Loss modulus

Loss modulus was measured in the temperature range 25–160 °C both during heating and cooling. Similar to the storage modulus, the values obtained in the cooling part of the curves were higher compared to those of the heating run; so the data points obtained from the cooling part were used in the following analysis.

The loss modulus versus temperature plots of the PA6-Boehmite and PA6-Ti-Boehmite samples are shown in Figs. 3 and 4, respectively.

When the results from both series are compared, some interesting features are found. The most interesting observation is related to the peak temperatures of the loss modulus curves. The peak temperature reflects the glass transition temperature of the polymer matrix. Although the polymer matrix is the same in both cases, the slight difference in the filler composition creates a difference in polymer dynamics, and as a result, in the glass transition temperatures (T_g). T_g values of the PA6-Boehmite samples are variable in the range of 48–52 °C and they do not follow any clear trend. On the other hand, the PA6-Ti-Boehmite samples have T_g values in the range of 45–50 °C, which are slightly lower compared to the PA6-Boehmite series. These values seem to have a clear trend with filler concentration: the T_g values start from 49 °C, gradually decrease until 45 °C at 3 and 5.5% Ti-Boehmite contents and then increase again with filler concentration. Obviously, the plasticizing effect of

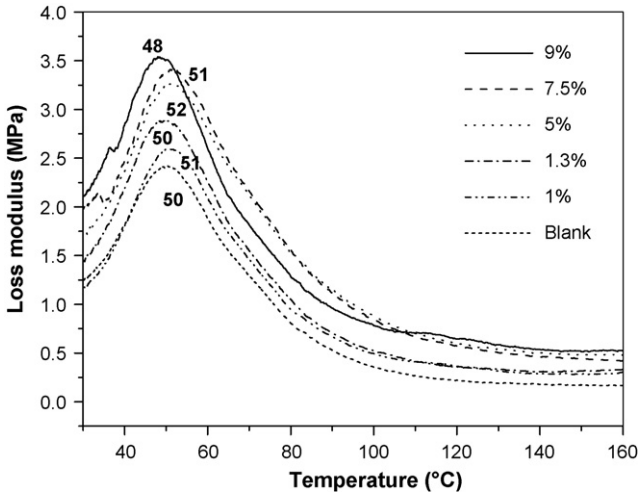

Fig. 3. Loss modulus E'' curves of PA6-Boehmite samples in the temperature range 35–160 °C, measured at 1 Hz. The glass transition temperatures (peak temperatures) are indicated in the figure.

the titanate-coupling agent plays an important role in lowering the T_g values at concentrations for which the HDT values are also lower (1–5.5% filler contents).

3.3. Complex Halpin–Tsai model

So far, many different models have been used in the literature to understand the mechanical behavior of polymer nanocomposites. In our previous work using the same systems (PA6-(Ti-)Boehmite), the Halpin–Tsai model (1) was found to be in good agreement with the experimental results. The model was originally developed to describe the mechanical properties of semi-crystalline polymers [13,14].

$$\frac{E_c}{E_m} = \frac{1 + \varsigma\eta\phi_f}{1 - \eta\phi_f} \quad \text{in which} \quad \eta = \frac{(E_f/E_m) - 1}{(E_f/E_m) + \varsigma} \tag{1}$$

where E_c is the composite Young's modulus; E_f is the filler modulus; E_m is the matrix modulus; ζ is the shape factor—depending on geometry, aspect ratio and orientation; ϕ_f is the filler volume fraction. Similar expressions can be derived for other types of modulus.With the appropriate shape factors for different particle shapes and orientations, this model can successfully describe Young's and shear modulus. The specific shape factors can be determined by comparing the model with experimental results or with more fundamental theories like Eshelby theory, Mori–Tanaka theory and 3D finite element modelling [15–17].

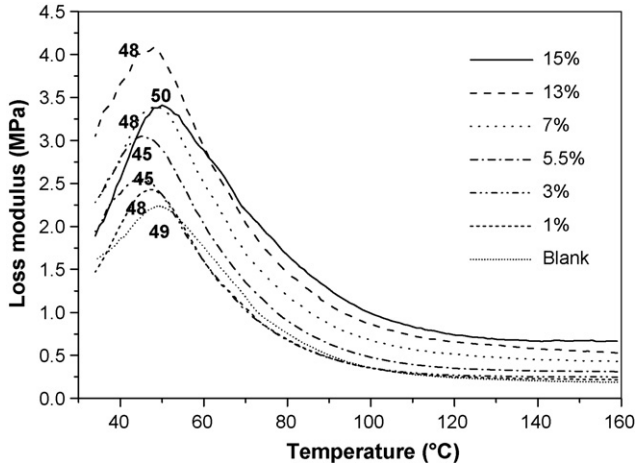

Fig. 4. Loss modulus E'' curves of PA6-Ti-Boehmite samples in the temperature range 35–160 °C, measured at 1 Hz. The glass transition temperatures (peak temperatures) are indicated in the figure.

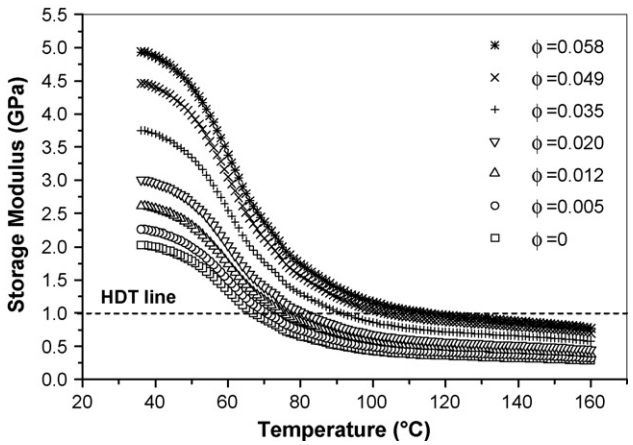

Fig. 5. Storage modulus E' curves derived from the Halpin–Tsai model.

The shape factors for fibres and rods (a is the length; b is the width) are [16]:

E_{11} or E_{22} $\quad \varsigma = 2$ $\quad$ (perpendicular to the fibre direction)

E_{33} $\quad \varsigma = 2\left(\frac{a}{b}\right)$ $\quad$ (in the fibre direction)

The Halpin–Tsai equations predict that particles are hardly effective at very low aspect ratios (<10). The maximum stiffening effect is reached only at aspect ratios above 1000 for platelets and 100 for fibres [17].

As mentioned earlier, our previous work used the Halpin–Tsai model to explain the storage modulus dependence of the PA6-(Ti-)Boehmite nanocomposites on Boehmite concentration at room temperature. The present paper utilizes the same model in a broader sense; that is, for predicting the storage and loss modulus values, both as a function of filler concentration and temperature. This approach allows one to extract additional information from the modulus curves, such as heat distortion and glass transition temperatures. A similar approach was taken by Fornes and Paul in a study where Halpin–Tsai predictions for storage modulus as a function of temperature were used to derive the HDTs [18]. Our method uses the complex number version of the Halpin–Tsai model written in an excel program as is justified by the analytic continuation theorem. The storage and loss modulus of the unfilled polymer measured as a function of temperature together with the storage modulus of the filler are substituted into the equations. It is assumed that the loss modulus of an inorganic filler is zero, because it is purely elastic. The Young's (storage) modulus of Boehmite is taken as 253 GPa [19]. In order to convert weight percentages to volume fractions, 1.13 and 3.01 g/cm^3 [20] have been used for the densities of polyamide-6 and Boehmite, respectively. The excel program defines the complex modulus of the matrix and the filler as $E_m = E'_m + iE''_m$ and $E_f = E'_f + iE''_f$ and uses them to calculate the complex modulus of the composite as $E_c = E'_c + iE''_c$. (It should be noted that E''_f is taken to be zero.) The output can be separated into the storage (E'_c) and the loss (E''_c) modulus of the (nano)composite.

Fig. 5 shows the storage modulus curves (E'_c) obtained from the complex Halpin–Tsai model as a function of temperature and Boehmite volume fraction. These curves show close resemblance to the experimental curves in Figs. 1 and 2, although the maximum storage modulus predicted by the model (4.93 GPa) is slightly

Table 2
Heat distortion temperatures derived from the Halpin–Tsai model

Boehmite vol. fraction	Corresponding to sample	HDT at 1 GPa (°C)
0	PA6-unfilled	67
0.005	PA6-Boeh 1.3%	71
0.012	PA6-Ti-Boeh 3%	75
0.020	PA6-Ti-Boeh 5.5%	81
0.035	PA6-Boeh 9%	91
0.049	PA6-Ti-Boeh 13%	103
0.058	PA6-Ti-Boeh 15%	116

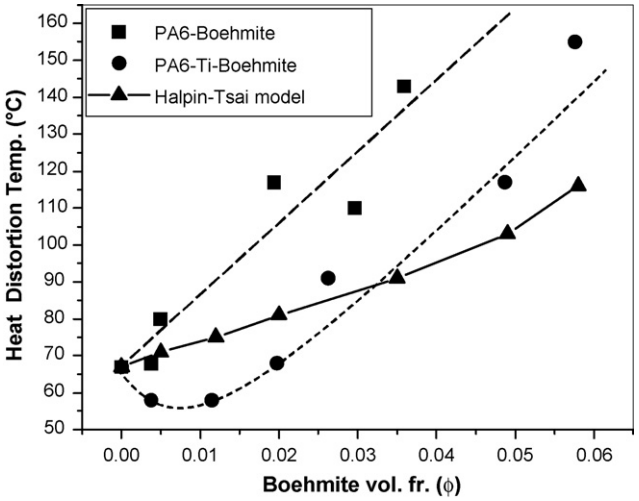

Fig. 6. Heat distortion temperatures of the nanocomposites as a function of Boehmite volume fraction.

higher than the actual value (4.23 GPa). The HDT values extracted from Fig. 5 are presented in Table 2 and plotted together with the experimental HDT values in Fig. 6. Loss modulus curves (E_c'') that are also obtained from the model, are displayed in Fig. 7 as a function of temperature and Boehmite volume fraction.

As seen in Fig. 6, the experimental HDT values for both types of nanocomposites have a linear dependence on Boehmite volume fraction. PA6-Ti-Boehmite samples show a slight deviation from linearity at low filler contents, which is attributed to the plasticizing effect of the titanate-coupling agent. Despite this deviation in the beginning, linear fitting of the experimental results yields plots that have identical slopes (indicated by dashed lines). The

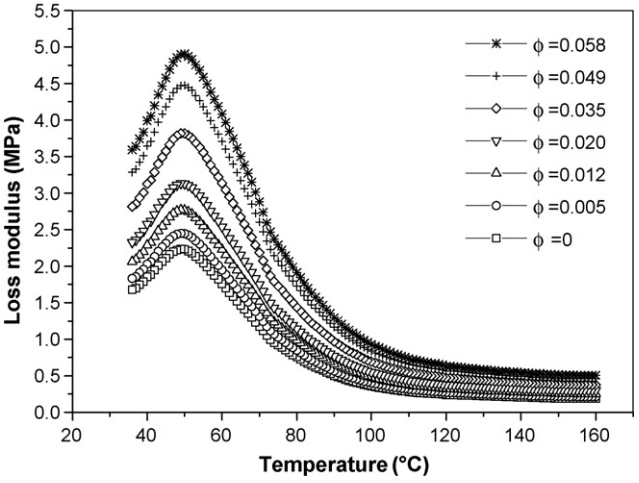

Fig. 7. Loss modulus E'' curves derived from the Halpin–Tsai model.

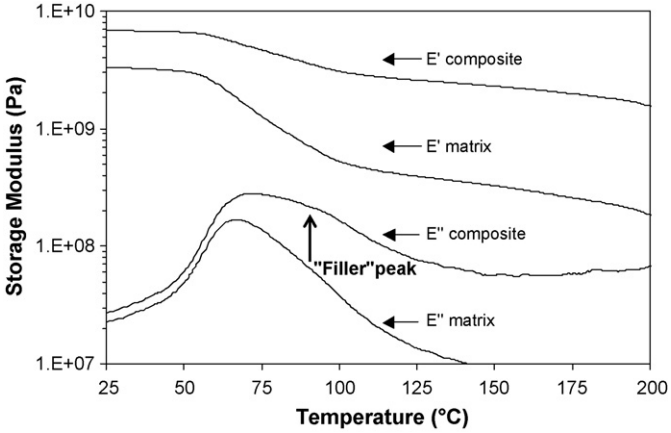

Fig. 8. Calculated storage and loss moduli based on the measured data for the polymer matrix for the composite (E_c' and E_c'') and the polymer matrix (E_m' and E_m'') using $\zeta = 500$ and $\phi_f = 0.03$ (the figure is taken from Ref. [20]).

plot obtained from the Halpin–Tsai model (indicated by the broken line) also follows a linear increase, however, with a lower slope compared to the experimental plots. Apart from the initial deviation in the PA6-Ti-Boehmite data points, it is possible to claim that the experimental HDT values are higher than those predicted by the model. This may originate from the fact that the Halpin–Tsai model is based on purely mechanical considerations and does not take Boehmite–Boehmite or Boehmite–polymer interactions into account, which may play an important role in HDT (for instance, bridging of the particles). Although Boehmite particles have lower L/D ratios compared to conventional clay type fillers, they seem to contribute more effectively to the thermo-mechanical stability of the polymer than that is predicted by the Halpin–Tsai model.

Fig. 7 shows the loss modulus E'' curves derived from the Halpin–Tsai model. Here, the glass transition temperatures (T_g) reflected by the peak points in the loss modulus, do not change significantly with filler concentration. The T_g values are predicted as 49 °C in the beginning and they are expected to shift to 50 °C at the highest concentrations (volume fractions of 0.035 and above). In other words, the model predicts a constant T_g behavior for the system and does not explain the variation in the experimental T_gs. According to Picken et al., the Halpin–Tsai model itself may give rise to an additional relaxation peak at higher temperatures [21]. When the equations in (1) are rewritten as one equation, the physical nature of the model becomes more obvious. The appearance of the normal relaxation (loss) peak results from the changing polymer matrix dynamics at T_g, whereas the second high temperature peak results from the transition from “parallel” to “series”-like mechanical behavior and is explained in terms of the pre-factors in the recombined Halpin–Tsai equations (Fig. 8). The second “filler-peak” only turns up at rather high aspect ratios ($\zeta > 500$) and is not expected to be visible in the present experiments, especially considering the particle polydispersity. However, at practical aspect ratios, this effect may cause an *apparent* rise of the T_g of the composite due to partial overlap of the polymer peak and the “filler-peak”. Vlasveld et al. have partially observed this effect in their nanocomposites reflected by the asymmetric broadening of the loss modulus peaks [22]. With the present system, the loss modulus E'' curves derived from the model reveal broader peaks at volume fractions of 0.035 and above (Fig. 7). Likewise, the experimental E'' curves in Figs. 3 and 4 show broadened peaks at high volume fractions. However, the overall effect of the Boehmite particles on the E'' curves in terms of peak-broadening is small due to their moderate aspect ratios ($\zeta = 28$).

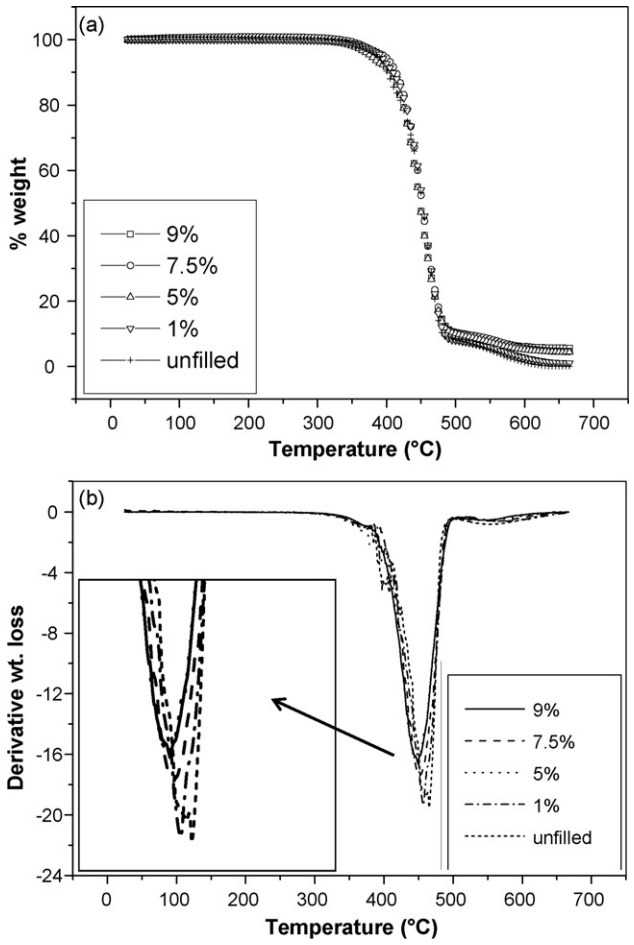

Fig. 9. (a) TGA curves of PA6-Boehmite samples in the temperature range 25–700 °C. (b) First derivative of the TGA curves of PA6-Boehmite samples in the temperature range 25–700 °C (the inset shows the area of interest).

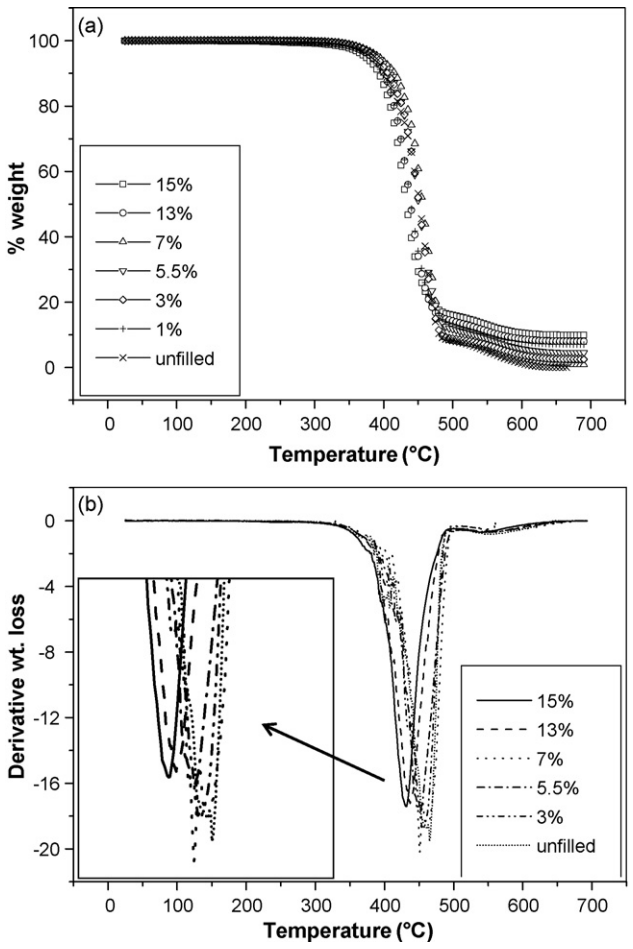

Fig. 10. (a) TGA curves of PA6-Ti-Boehmite samples in the temperature range 25–700 °C. (b) First derivative of the TGA curves of PA6-Ti-Boehmite samples in the temperature range 25–700 °C (the inset shows the area of interest).

3.4. Thermo-oxidative stability

As indicated in Section 2.3, thermo-oxidative stabilities were determined by TGA in a temperature range of 25–700 °C. Figs. 9a and 10a show the TGA curves of PA6-Boehmite and PA6-Ti-Boehmite samples, respectively. According to these curves, the thermo-oxidative stabilities of the nanocomposites with modified or unmodified Boehmite are similar, although the degradation starts slightly earlier at high Ti-Boehmite contents (13 and 15%). The part of the curves in the range 500–700 °C shifts systematically upwards with filler concentration, which is an expected trend. Since most of the polymer has degraded by these temperatures, the amount of sample residue is directly proportional to Boehmite content. Since the TGA weight loss curves of PA6-Boehmite and PA6-Ti-Boehmite samples look identical, the first derivatives of these curves are investigated for more detailed information.

Figs. 9b and 10b show the first derivative of the TGA curves of PA6-Boehmite and PA6-Ti-Boehmite samples, respectively. The peak minima correspond to the point of maximum weight loss. As seen in these figures, the temperatures at which the maximum weight loss occurs, shifts to lower values with increased filler concentration. The amount of shift is more pronounced with the PA6-Ti-Boehmite system due to the presence of samples with higher filler contents. For a detailed comparison, the temperatures corresponding to 10% and maximum weight loss of PA6-Boehmite and PA6-Ti-Boehmite samples are presented in Table 3. According to Table 3, the temperatures of 10% weight loss do not contain relevant information. Both type of nanocomposites follow a similar trend in the sense that the temperatures at 10% weight loss are slightly higher than that of the unfilled polymer. On the other hand, the temperatures of maximum weight loss show more clear trends: they shift to lower values with increasing filler content. These values are similar for both types of samples with comparable Boehmite and Ti-Boehmite contents. According to this, it can be concluded that both type of nanocomposites have similar thermo-oxidative stabilities. This suggests that the lower T_g and HDT values of the PA6-Ti-Boehmite samples originate from the

Table 3
Temperatures corresponding to 10% and maximum weight loss of PA6-Boehmite and PA6-Ti-Boehmite samples

Sample	*T* at 90%	*T* at maximum wt. loss
PA6-Boeh 1%	409	457
PA6-Boeh 5%	406	447
PA6-Boeh 7.5%	414	451
PA6-Boeh 9%	409	449
PA6-unfilled	400	465
PA6-Ti-Boeh 3%	405	457
PA6-Ti-Boeh 5.5%	409	452
PA6-Ti-Boeh 7%	416	451
PA6-Ti-Boeh 13%	400	437
PA6-Ti-Boeh 15%	393	431

effect of plasticization on the local polymer dynamics and softening of the polymer–filler interface, and not from the plasticization of the system due to the presence of volatile substances (i.e., unreacted surface-modifier).

4. Conclusions

The present work focuses on the thermo-mechanical behavior of (Ti-)Boehmite-polyamide-6 system. According to that, storage and loss moduli increase gradually with (Ti-)Boehmite concentration. There is a tremendous increase in HDT starting from that of the unfilled polymer (67 °C), up to 143 °C and 155 °C of PA6-Boehmite and PA6-Ti-Boehmite, respectively. PA6-Boehmite samples show a random variation in glass transition temperatures (T_g) whereas the PA6-Ti-Boehmite system shows a clear trend with filler concentration: the T_g values decrease gradually in the beginning, then increase again with filler concentration. It is also shown that both types of Boehmite impart comparable thermo-oxidative stability to the polymer. This implies that the lower initial values of T_g and HDT in PA6-Ti-Boehmite nanocomposites are caused by the changes in interfacial (polymer) dynamics, and not due to the plasticization from some unreacted titanate-coupling agent. The Halpin–Tsai model is used to predict the heat distortion and glass transition temperatures. However, the model predicts a constant T_g behavior for the system and does not explain the variations in the experimental T_g values. It also predicts a linear increase for the HDTs with increasing (Ti-)Boehmite concentration, but with a slope lower than that of the experimental results. Apart from the initial decrease in the PA6-Ti-Boehmite data points, all experimental HDT's are higher than those predicted by the model. It is concluded that (Ti-)Boehmite particles contribute more effectively to the thermo-mechanical stability of the polymer than predicted by the Halpin–Tsai model. This is probably related to the fact that the Halpin–Tsai model is based on purely mechanical considerations and does not take Boehmite–Boehmite or Boehmite–polymer interactions into account.

Acknowledgement

The authors would like to thank the Dutch Polymer Institute for their financial support of the PhD work of Ceren Özdilek.

References

[1] S. Qutubuddin, X. Fu, in: M. Rosoff (Ed.), Nano-surface Chemistry, Marcel Dekker, Inc., New York, 2002, pp. 653–673.
[2] Y. Fukushima, S. Inagaki, J. Inclusion Phenom. 5 (1987) 473–482.
[3] A. Usuki, M. Kawasumi, Y. Kojima, A. Okada, T. Kurauchi, O. Kamigaito, J. Mater. Res. 8 (1993) 1174–1178.
[4] A. Usuki, Y. Kojima, M. Kawasumi, A. Okada, Y. Fukushima, T. Kurauchi, O. Kamigaito, J. Mater. Res. 8 (1993) 1179–1184.
[5] Y. Kojima, A. Usuki, M. Kawasumi, A. Okada, T. Kurauchi, O. Kamigaito, J. Appl. Polym. Sci. 49 (1993) 1259–1264.
[6] J.W. Gilman, T. Kashiwagi, J.D. Lichtenhan, SAMPE J. 33 (1997) 40–46.
[7] C. Özdilek, Colloidal Liquid Crystalline Reinforced Nanocomposites, Ph.D. Thesis, Delft University of Technology, Delft, 2006.
[8] C. Özdilek, K. Kazimierczak, D. van der Beek, S.J. Picken, Polymer 45 (2004) 5207–5214.
[9] C. Özdilek, K. Kazimierczak, S.J. Picken, Polymer 46 (2005) 6025–6034.
[10] P.A. Buining, C. Pathmamanoharan, J.B.H. Jansen, H.N.W. Lekkerkerker, J. Am. Ceram. Soc. 74 (1991) 1303–1307.
[11] A.K. van der Vegt, L.E. Govaert, Polymeren: Van Keten tot Kunststof, DUP Blue Print, Delft, 2003.
[12] Y. Kojima, A. Usuki, M. Kawasumi, A. Okada, Y. Fukushima, T. Kurauchi, O. Kamigaito, J. Mater. Res. 8 (1993) 1185–1189.
[13] J.C. Halpin, J.L. Kardos, Polym. Eng. Sci. 16 (1976) 344–352.
[14] J.C. Halpin, J. Compos. Mater. 3 (1969) 732–734.
[15] N. Sheng, M.C. Boyce, D.M. Parks, G.C. Rutledge, J.I. Abes, R.E. Cohen, Polymer 45 (2004) 487–506.
[16] M. van Es, F. Xiqiao, J. van Turnhout, E. van der Giessen, in: S. Al-Malaika, A. Golovoy, C.A. Wilkie (Eds.), Specialty Polymer Additives, Blackwell Science, Oxford, 2001.
[17] M. van Es, Polymer clay nanocomposites. The importance of particle dimensions, Ph.D. Thesis, Delft University of Technology, Delft, 2001.
[18] T.D. Fornes, D.R. Paul, Polymer 44 (2003) 4993–5013.
[19] M.R. Gallas, G.J. Piermarini, J. Am. Ceram. Soc. 77 (1994) 2917–2920.
[20] P.A. Buining, Preparation and properties of dispersions of colloidal Boehmite rods, Ph.D. Thesis, Utrecht University, Utrecht, 1992.
[21] S.J. Picken, D.P.N. Vlasveld, H.E.N. Bersee, C. Özdilek, E. Mendes, in: P. Knauth, J. Schoonman (Eds.), Nanocomposites: Ionic Conducting Materials and Structural Spectroscopies, Springer, 2007.
[22] D.P.N. Vlasveld, S.G. Vaidya, H.E.N. Bersee, S.J. Picken, Polymer 46 (2005) 3452–3461.